Supporting Information for

Tuning gas transport and separation in ZIF-8 membranes via point defects: insights from non-equilibrium molecular dynamics

Kexin Peng,[a,b] Shengtang Liu,[*c] Shitong Zhang,[*a,b] and Chongli Zhong[a,b]

[a]*State Key Laboratory of Advanced Separation Membrane Materials, Tiangong University, Tianjin 300387, China.*

[b]*School of Chemical Engineering, Tiangong University, Tianjin, 300387, PR China*

[c]*Institute of Quantitative Biology and Medicine, State Key Laboratory of Radiation Medicine and Protection, School of Radiation Medicine and Protection, Collaborative Innovation Center of Radiological Medicine of Jiangsu Higher Education Institutions, Soochow University, Jiangsu 215123, China.*

*Corresponding Author.

E-mail address: liushengtang@suda.edu.cn (S. Liu);

zhangshitong@tiangong.edu.cn (S. Zhang);

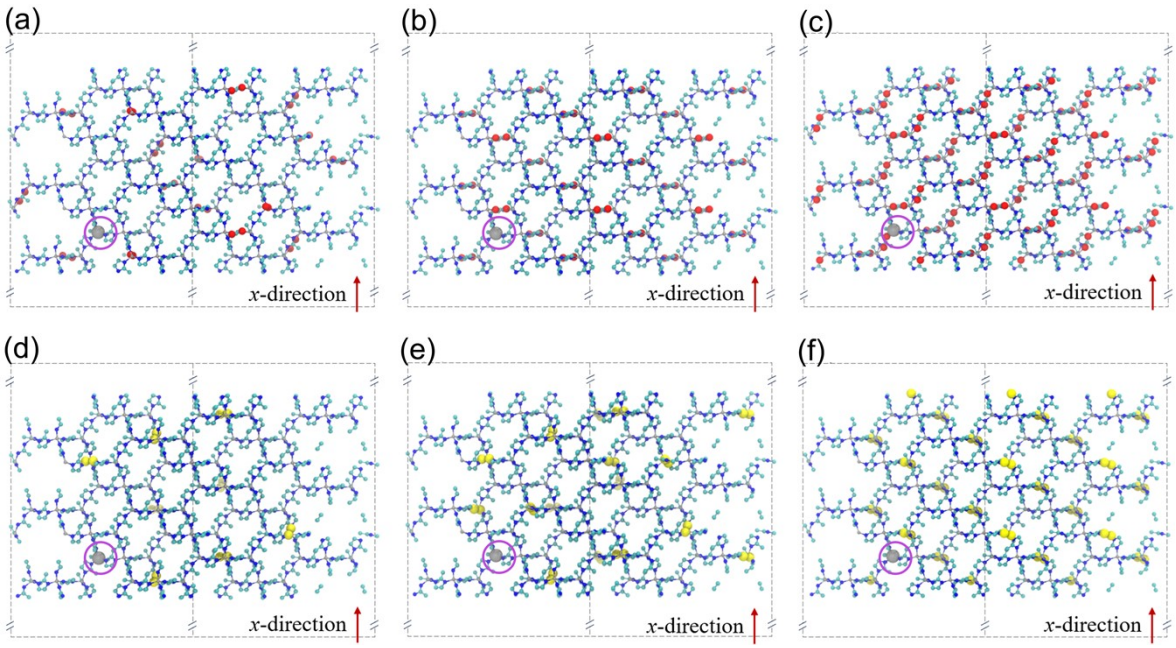

Fig. S1. Side-view structures of defective models: (a) LV-1, (b) LV-2, (c) LV-3, (d) ZnV-1, (e) ZnV-2, and (f) ZnV-3 (color code: white, H; cyan, C; blue, N; red, O; slate-grey, Zn). In panels (a–c), the oxygen atoms generated upon the formation of linker vacancies are displayed as red VDW spheres to indicate the defect sites. In panels (d–f), the tan VDW spheres represent the H atoms introduced as a result of missing Zn atoms, indicating the Zn vacancy sites. Other H atoms in all panels are not shown for the sake of clarity. The fixed Zn atom in each model is shown as a slate-grey VDW sphere (as highlighted by purple cycle).

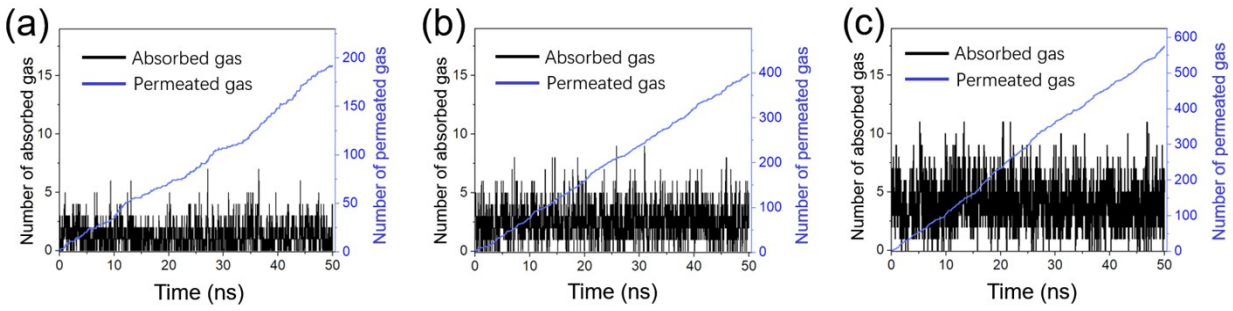

Fig. S2. The evolution of the absorbed and permeated gas numbers over simulation time with pressure drops of (a) 2 bar, (b) 4 bar, and (c) 6 bar.

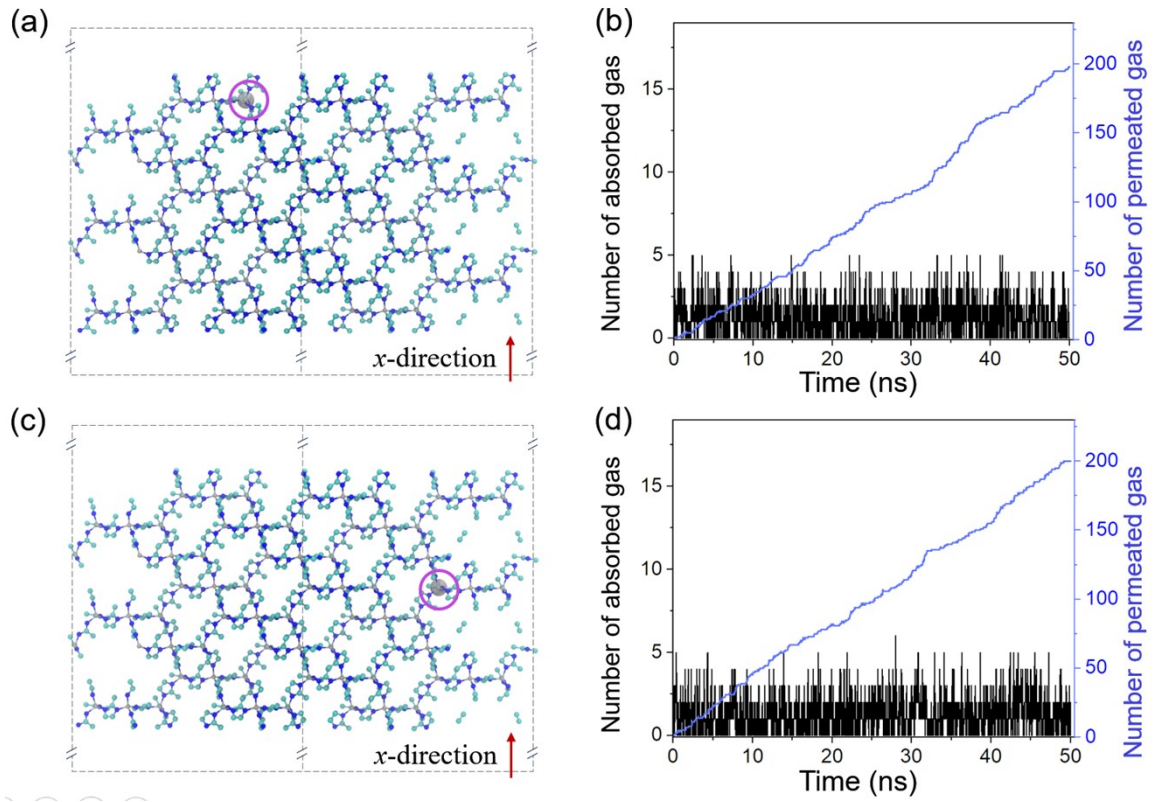

Fig. S3. (a) Pristine membrane models with a fixed Zn atom located near the permeate chamber, as highlighted by purple cycle; (b) time evolution of the absorbed and permeated numbers of He for the models shown in (a); (c) pristine membrane models with a fixed Zn atom located in the interior bulk region, as highlighted by purple cycle; (d) time evolution of the absorbed and permeated numbers of He for the models shown in (c). Compared with Fig. S2a, where the fixed Zn atom is located near the feed chamber, the He transport behaviors obtained from different fixation positions are in good agreement with each other.

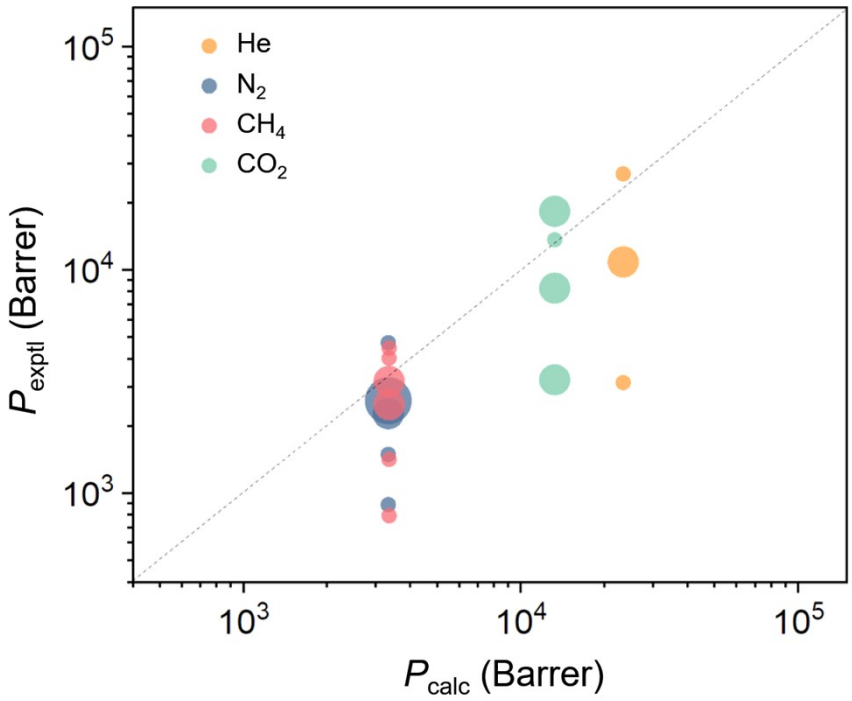

Fig. S4. Comparison between calculated gas permeabilities (P_{calc}) and reported experimental results (P_{exptl}).[1-10] Bubble size indicates the number of experimentally reported data points, with larger bubbles representing a greater count.

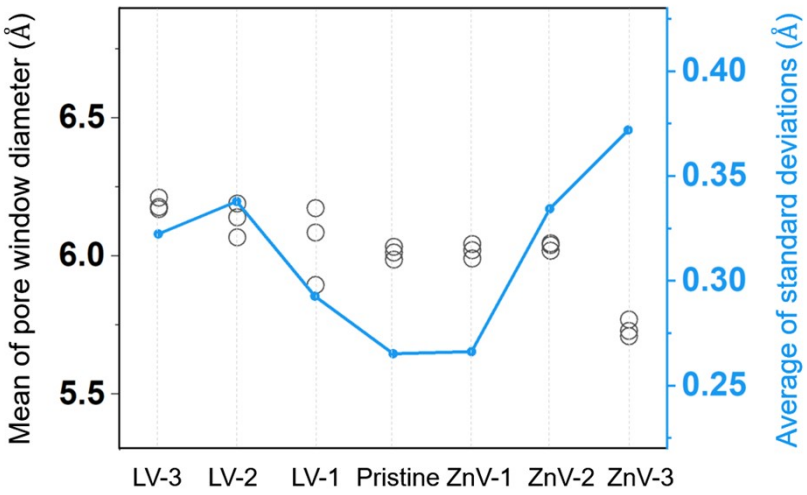

Fig. S5. Mean pore window diameter (defined as the distance between the two H atoms at the diagonal positions of the 6-membered-ring windows located at approximately x = ~216 Å) and the average of the corresponding standard deviations (blue line and symbols, right y-axis) for ZIF-8 membranes with different defect types and concentrations. Data were collected from a 5 ns MD simulation of membrane-only models. Higher standard deviation values indicate a more

pronounced fluctuation in the positions of the H atoms.

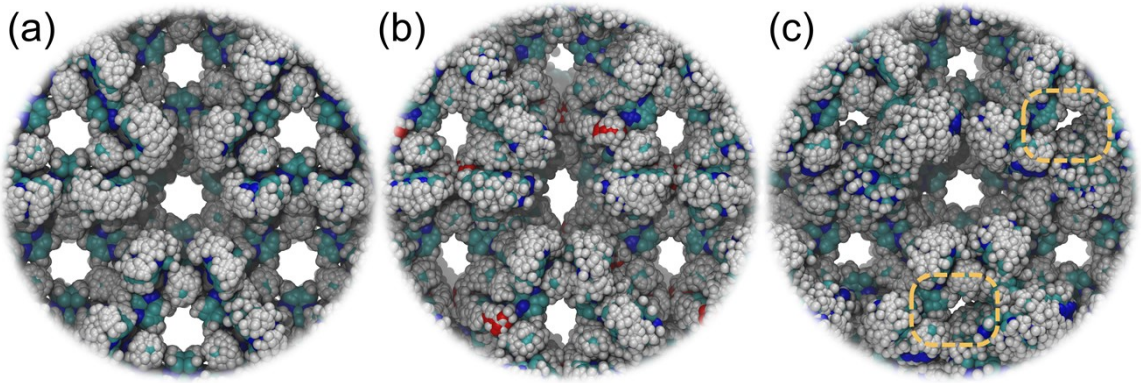

Fig. S6. Overlay of atomic positions sampled over a 5 ns MD trajectory for the (a) pristine, (b) LV-3 and (c)ZnV-3 membrane models; the broader positional clouds in ZnV-3 indicate greater linker mobility (yellow dashed circle) compared with the more rigid pristine and LV-3 frameworks.

Table S1. Non-bonded potential parameters for ZIF-8 membranes and graphene barrier layer.

Atom type	σ (nm)	ε (kJ/mol)	q (e)[a]	description
Zn	0.246	0.329	0.65	Zn in ZIF-8
N_R	0.326	0.183	−0.35, −0.32	N in ZIF-8
C_R	0.343	0.279	−0.08 – −0.01[b], 0.43[c]	C in imidazole ring
C_3	0.343	0.279	−0.47	C in methyl
C_G	0.343	0.150[d]	0	C in graphene barrier layer
H_1	0.257	0.117	0.09	H bonded to C_R
H_2	0.257	0.117	0.26	H bonded to N_R
H_3	0.257	0.117	0.13	H in methyl
H_O	0.257	0.117	0.35	H bonded to O
O_1	0.312	0.158	−0.67	O bonded to one H
O_2	0.312	0.158	−0.75	O bonded to two H

[a]This value represents the average charge calculated using the ML method; the point charges of individual atoms fluctuate by up to approximately 15%; in addition, the exact values are influenced by the defect type and defect concentration; more detailed data are not listed here due to the large amount of information. [b]Charge of C in the imidazole ring bonded to H. [c]Charge of C in the imidazole ring not bonded to H. [d]This value has been significantly reduced to lower the adsorption of gases by the barrier layer; it is therefore strongly discouraged to use it for other

simulations involving graphene properties.

Table S2. The employed force field parameters for gas molecules.

He	σ (nm)	ε (kJ/mol)	q (e)	ref[11]
He	0.264	0.091	0	
CH_4	σ (nm)	ε (kJ/mol)	q (e)	ref[12]
C_met	0.373	1.230	0	
N_2	σ (nm)	ε (kJ/mol)	q (e)	ref[13]
N_n	0.331	0.303	−0.48	
N_m	0	0	0.96	
bond-term	k (kJ/(mol·nm²))		r_0 (nm)	
N_n–N_n	Fixed length		0.110	
CO_2	σ (nm)	ε (kJ/mol)	q (e)	ref[13][14]
C	0.280	0.234	0.70	
O	0.302	0.668	−0.35	
bond-term	k (kJ/(mol·nm^2))		r_0 (nm)	
C–O	844300.0		0.116	
angle-term	k (kJ/(mol·rad^2))		θ_0	
O–C–O	451.9		180.0°	

References

1. C. Zhang, R. P. Lively, K. Zhang, J. R. Johnson, O. Karvan and W. J. Koros, Unexpected molecular sieving properties of zeolitic imidazolate framework-8, *J. Phys. Chem. Lett.*, 2012, **3**, 2130-2134.
2. N. Hara, M. Yoshimune, H. Negishi, K. Haraya, S. Hara and T. Yamaguchi, Diffusive separation of propylene/propane with ZIF-8 membranes, *J. Membr. Sci.*, 2014, **450**, 215-223.
3. M. Drobek, M. Bechelany, C. Vallicari, A. Abou Chaaya, C. Charmette, C. Salvador-Levehang, P. Miele and A. Julbe, An innovative approach for the preparation of confined ZIF-8 membranes by conversion of ZnO ALD layers, *J. Membr. Sci.*, 2015, **475**, 39-46.
4. N. Hara, M. Yoshimune, H. Negishi, K. Haraya, S. Hara and T. Yamaguchi, ZIF-8 membranes prepared at miscible and immiscible liquid–liquid interfaces, *Microporous Mesoporous Mater.*, 2015, **206**, 75-80.
5. K. Tao, C. Kong and L. Chen, High performance ZIF-8 molecular sieve membrane on hollow ceramic fiber via crystallizing-rubbing seed deposition, *Chem. Eng. J.*, 2013, **220**, 1-5.
6. M. Shah, H. T. Kwon, V. Tran, S. Sachdeva and H.-K. Jeong, One step in situ synthesis of supported zeolitic imidazolate framework ZIF-8 membranes: Role of sodium formate, *Microporous Mesoporous Mater.*, 2013, **165**, 63-69.
7. X. Wang, M. Sun, B. Meng, X. Tan, J. Liu, S. Wang and S. Liu, Formation of continuous and highly

permeable ZIF-8 membranes on porous alumina and zinc oxide hollow fibers, *Chem. Commun.*, 2016, **52**, 13448-13451.

8. K. Tao, L. Cao, Y. Lin, C. Kong and L. Chen, A hollow ceramic fiber supported ZIF-8 membrane with enhanced gas separation performance prepared by hot dip-coating seeding, *J. Mater. Chem. A*, 2013, **1**, 13046-13049.
9. M. C. McCarthy, V. Varela-Guerrero, G. V. Barnett and H.-K. Jeong, Synthesis of zeolitic imidazolate framework films and membranes with controlled microstructures, *Langmuir*, 2010, **26**, 14636-14641.
10. X. Zhang, Y. Liu, L. Kong, H. Liu, J. Qiu, W. Han, L.-T. Weng, K. L. Yeung and W. Zhu, A simple and scalable method for preparing low-defect ZIF-8 tubular membranes, *J. Mater. Chem. A*, 2013, **1**, 10635-10638.
11. J. O. Hirschfelder, C. F. Curtiss and R. B. Bird, *Molecular theory of gases and fluids*, Wiley, New York, 1954.
12. M. G. Martin and J. I. Siepmann, Transferable potentials for phase equilibria. 1. United-atom description of n-alkanes, *J. Phys. Chem. B*, 1998, **102**, 2569-2577.
13. X. Wu, J. Huang, W. Cai and M. Jaroniec, Force field for ZIF-8 flexible frameworks: atomistic simulation of adsorption, diffusion of pure gases as CH_4, H_2, CO_2 and N_2, *Rsc Adv.*, 2014, **4**, 16503-16511.
14. S. M. Khan, H. Kitayama, Y. Yamada, S. Gohda, H. Ono, D. Umeda, K. Abe, K. Hata and T. Ohba, High CO_2 sensitivity and reversibility on nitrogen-containing polymer by remarkable CO_2 adsorption on nitrogen sites, *J. Phys. Chem. C*, 2018, **122**, 24143-24149.